Applied Catalysis B: Environmental 224 (2018) 410–418

Contents lists available at ScienceDirect

Applied Catalysis B: Environmental

journal homepage: www.elsevier.com/locate/apcatb

Research Paper

Solar photoelectro-Fenton treatment of a mixture of parabens spiked into secondary treated wastewater effluent at low input current

Juliana R. Steter, Enric Brillas, Ignasi Sirés*

Laboratori d'Electroquímica dels Materials i del Medi Ambient, Departament de Química Física, Facultat de Química, Universitat de Barcelona, Martí i Franquès 1-11, 08028 Barcelona, Spain

ARTICLE INFO

Keywords:
Boron-doped diamond
Dimensionally stable anode
Parabens
Solar photoelectro-Fenton
Wastewater treatment

ABSTRACT

Aqueous mixtures of methyl, ethyl and propyl paraben (MeP, EtP and PrP) prepared in real urban wastewater with low conductivity were treated by solar photoelectro-Fenton (SPEF) process at low input current (j = 10 mA cm^{-2}) using a pre-pilot plant with an electrochemical reactor equipped with an air-diffusion cathode to electrogenerate H_2O_2 and a boron-doped diamond (BDD) or RuO_2-based anode. Comparative trials in simulated water matrices with or without Cl^- in the absence of natural organic matter (NOM) always led to a slower decay of parabens concentration and total organic carbon (TOC). This was mainly due to the superior regeneration of Fe^{2+} from photoreduction of Fe(III) complexes formed with NOM in real wastewater compared to that from $Fe(OH)^{2+}$. In all matrices, a catalyst concentration as low as 0.20 mM Fe^{2+} was enough to ensure the production of ·OH in the bulk from Fenton's reaction. SPEF with BDD yielded a complete removal of parabens in 180 min and 66% mineralization at 240 min. This gave rise to the greatest mineralization current efficiencies reported so far, up to 1000%, with a low energy consumption of 84 kWh (kg TOC)$^{-1}$. The synergy between homogeneous and heterogeneous catalysis, which allowed the efficient dosage of ·OH and M(·OH) at low j, with simultaneous action of high UV power from sunlight justified such a good performance. Analogous apparent rate constants were determined for MeP, EtP and PrP. Slower decays were found with RuO_2-based anode due to its lower oxidation power. As a result, the MCE was 425% as maximum, but a lower energy consumption of 52 kWh (kg TOC)$^{-1}$ was needed. Since the role of active chlorine was of minor importance, the formation of toxic, refractory chloroderivatives was minimized. All by-products were transformed into malic, formic and oxalic acids prior to total mineralization.

1. Introduction

In recent years, the electrochemical technologies for the removal of man-made organic contaminants from water bodies have seen an extraordinary development, in parallel to the progressively greater environmental and health concerns associated to xenobiotics. In particular, major interest is focused on two kinds of electrochemical advanced oxidation processes (EAOPs) that allow, in many cases, the total transformation of the parent pollutants into innocuous by-products: electro-oxidation (EO) and Fenton-based EAOPs like electro-Fenton (EF) and UVA or solar photoelectro-Fenton (PEF or SPEF) [1].

EO is the simplest EAOP for treating organic pollutants, since it relies on the promotion of heterogeneous catalysis at the surface of a suitable anode (M), yielding adsorbed hydroxyl radicals (·OH) from water oxidation as follows:

$$M + H_2O \rightarrow M(\cdot OH) + H^+ + e^- \quad (1)$$

Boron-doped diamond (BDD) exhibits the highest performance in EO owing to its large overpotential for O_2 evolution [2], but it presents some shortcomings like high cost, electrode instability during wastewater treatment and difficulties to fabricate large electrodes [3]. This has led to the alternative use of metal oxides as dimensionally stable anodes, which allow the removal of recalcitrant chemicals at a much lower cost [4]. However, the relationship between the surface structure of metal oxides and their electrocatalytic ability is not so clear as in the case of BDD and hence, results tend to be case-sensitive. In contrast to non-active BDD anode, it has been established that the radical M(·OH) formed from Reaction (1) on the surface of active metal oxides is partially transformed into the weaker oxidant MO, thus conferring to the anode a lower oxidation ability. But, in some cases, the enhanced adsorption of organics on the surface of metal oxides can improve the degradation process [1].

Low amounts of less powerful oxidants like O_3 and $S_2O_8^{2-}$ may be formed in concomitance with M(·OH). Some authors have combined

* Corresponding author.
E-mail address: i.sires@ub.edu (I. Sirés).

http://dx.doi.org/10.1016/j.apcatb.2017.10.060
Received 2 September 2017; Received in revised form 18 October 2017; Accepted 26 October 2017
Available online 27 October 2017

conventional EO with cathodic electrogeneration of H_2O_2 from two-electron reduction of O_2 according to Reaction (2), giving rise to the EO-H_2O_2 process [1]:

$$O_{2(g)} + 2H^+ + 2e^- \rightarrow H_2O_2 \quad (2)$$

The effectiveness of EO-H_2O_2 can be substantially enhanced upon homogeneous catalysis with metal cations like Fe^{2+} at pH ~ 3.0 [5]. In EF, H_2O_2 formed via Reaction (2) reacts with added Fe^{2+} according to Fenton's Reaction (3). Further enhancement is reached in PEF or SPEF under UVA irradiation, which maintains the catalytic cycle by promoting the continuous photolytic reduction of Fe(III) species via photo-Fenton Reaction (4).

$$H_2O_2 + Fe^{2+} \rightarrow Fe^{3+} + {}^{\bullet}OH + OH^- \quad (3)$$

$$Fe(OH)^{2+} + h\nu \rightarrow Fe^{2+} + {}^{\bullet}OH \quad (4)$$

Carbon-based cathodes are optimum to carry out EF, PEF and SPEF because they allow the efficient production of H_2O_2 at a low cost and toxicity. Among them, carbon felt [6–10] and air-diffusion electrodes [11–17] have been widely explored, being reticulated vitreous carbon [18,19] and BDD [20] more rarely employed.

At present, SPEF with air-diffusion cathode is the best option to mineralize organic pollutants at acidic pH, which can be explained by the large amount of H_2O_2 formed from Reaction (2) and the high UV power of sunlight compared to commercial UVA lamps [21–29]. The effectiveness of SPEF has been demonstrated by treating model organic pollutants such as pesticides [21], dyes [22–25], pharmaceuticals [26,27] and phytochemicals [28], as well as real landfill leachate [29]. In all these cases, the high conductivity of treated solutions favored the application of high current densities ($\gg > 33$ mA cm^{-2}), thus accelerating the degradation to the detriment of current efficiency. However, the performance of SPEF in real water matrices with low conductivity has not been reported yet. Furthermore, such samples usually contain Cl^-, which is plausibly oxidized to active chlorine (Cl_2, HClO and/or ClO^-) that competes with M($^{\bullet}$OH) and $^{\bullet}$OH formed at the anode and in the bulk, respectively [30–32].

Nowadays, parabens are organic pollutants of major concern because they act as endocrine disruptors [33] and may cause human cancers and dermatitis [34,35]. They are ubiquitous in our daily lives since they are widely used as antimicrobial preservatives in processed food, medicines, cosmetics and toiletries [36,37], despite the increasing restrictions worldwide. As a result of their widespread use along with their facile dispersion and bioaccumulation in the environment [38], the occurrence in effluents of municipal wastewater treatment facilities (WWTFs) has been documented [39], thus being necessary to develop more effective and efficient water reclamation technologies. Advanced treatment of parabens in water with mediation of hydroxyl radicals produced on site has been performed by O_3-based methods [40], Fenton process [41,42], and UVA or solar photocatalysis with TiO_2 [43,44]. A more efficient degradation has been reported by EAOPs like EO with BDD anode [45–47], as well as EF or PEF with UVA light [48]. These previous studies were focused on methyl paraben (MeP) in high conductivity media using high current densities.

This article pesents the degradation of a mixture of three parabens, namely methyl (MeP), ethyl (EtP) and propyl (PrP) paraben dissolved in urban wastewater with low conductivity (~ 3 mS cm^{-1}). Solutions of 2.5 L have been treated in batch mode, employing a pre-pilot plant including a photoreactor and an undivided filter-press cell equipped with a BDD or RuO_2-based anode and an air-diffusion cathode. Most of the experiments have been performed under SPEF conditions at low current density (j) of 10 mA cm^{-2}. The effect of j and parabens and iron concentrations has also been assessed. For comparison, EO, EF and SPEF trials in synthetic solutions prepared with Milli-Q water have been made as well. The performance of each treatment has been interpreted from TOC abatement, parabens decay, current efficiency profiles and energy consumption. The main primary reaction by-products and final aliphatic carboxylic acids have been identified by chromatographic techniques.

2. Materials and methods

2.1. Chemicals

MeP, EtP and PrP with ≥99% purity were supplied by Sigma-Aldrich. Anhydrous sodium sulfate used as supporting electrolyte and iron(II) sulfate heptahydrate used as catalyst in EF and SPEF were of analytical grade from Fluka. Analytical grade sulfuric acid from Merck was used to adjust the solution pH to 3.0. All other chemicals were of high performance liquid chromatography (HPLC) or analytical grade from Panreac and Sigma-Aldrich. Synthetic solutions were prepared with ultrapure water from a Millipore Milli-Q system.

2.2. Aqueous media

Parabens to be degraded were spiked into three different water matrices:

(i) A solution with 5 mM Na_2SO_4 in deionized water, with conductivity of 1.70 mS cm^{-1}.
(ii) A simulated water matrix (SWM) prepared with deionized water and containing the main ions that are typically found in WWTFs (Na^+, NH_4^+, SO_4^{2-}, Cl^-, NO_2^- and NO_3^-), but in the absence of natural organic matter, yielding a conductivity of 1.75 mS cm^{-1}.
(iii) Real wastewater (RWW) obtained from the secondary decanter of a municipal WWTF near Barcelona. The sample, which was kept at 4 °C all the time before use, contained 81.1 mg L^{-1} of total carbon and 10.8 mg L^{-1} of total organic carbon (TOC), its pH was 8.1 and its conductivity was 2.20 mS cm^{-1}. Cations included 0.20 mg L^{-1} Fe^{2+}, 33.6 mg L^{-1} K^+, 211.7 mg L^{-1} Na^+ and 36.9 mg L^{-1} NH_4^+, apart from traces of Ca^{2+} and Mg^{2+}. Anions included 0.79 mg L^{-1} NO_2^-, 0.85 mg L^{-1} NO_3^-, 318.0 mg L^{-1} Cl^- and 141.3 mg L^{-1} SO_4^{2-}.

Upon pH adjustment to 3.0, the final conductivity slightly increased up to 1.75, 1.80 and 3.70 mS cm^{-1}, respectively. Almost all the electrolyses were made with mixtures of 0.30 mM MeP + 0.30 mM EtP + 0.30 mM PrP (initial TOC content of 100 mg L^{-1}).

2.3. Bulk electrolyses

A flow plant operating in batch mode was employed to treat solutions of 2.5 L containing equimolar mixtures of the three parabens [23]. The solution, kept into a plastic reservoir, was continuously recirculated at a fixed flow rate of 180 L h^{-1} using a centrifugal pump, and maintaining a constant temperature of 30 °C by means of two heat exchangers. The solution entered into a filter-press electrochemical cell equipped with a 20 cm^2 BDD anode from NeoCoat or RuO_2-based plate from NMT Electrodes, along with a 20 cm^2 carbon-PTFE air-diffusion cathode from E-TEK, with an interelectrode gap of 1.2 cm. The cathode was prepared by painting a carbon cloth with the wet paste resulting from an equimass mixture of Vulcan XC-72 conductive specialty carbon black and 30-N PTFE dispersion in water, followed by compression at 350 °C for 30 min. The dry face of the cathode was fed with air through a gas chamber at an overpressure of about 8.6 kPa regulated with a back-pressure gauge, thus ensuring the continuous H_2O_2 production at the wet face from O_2 reduction on the carbon catalyst. The cell outlet was connected to a planar solar photoreactor of 600 mL capacity for the SPEF trials, which was covered with an opaque cloth in the EO-H_2O_2 and EF trials. A constant current was supplied by an Agilent 6552A DC power source, which displayed the cell voltage (E_{cell}) as well. The photoreactor was tilted 41° (latitude of facilities in Barcelona) to collect most of the direct sun rays. SPEF assays were carried out in sunny days

during the summer of 2016 and the natural UV irradiance (300–400 nm) was about 30–35 W m^{-2}, as determined with a Kipp & Zonen CUV 5 radiometer. The assays were typically carried out for 240 min, since longer electrolyses entailed a remarkable decrease of irradiance.

2.4. Instruments and analytical methods

The conductivity in each medium was determined from the electrical conductance measured on a Metrohm 644 conductometer, whereas the solution pH was measured on a Crison GLP 22 pH-meter. For all subsequent analyses, samples were filtered using 0.45 μm PTFE syringe filters from Whatman. The H_2O_2 and active chlorine contents accumulated from *in situ* electrogeneration were determined from the absorbance values obtained at λ = 408 and 515 nm, respectively, employing a Shimadzu 1800 UV/Vis spectrophotometer at 25 °C according to the Ti(IV) complexation and *N,N*-diethyl-*p*-phenylenediamine colorimetric methods [49,50]. The NH_4^+ content was evaluated through the indophenol blue method using the same spectrophotometer. The concentration of all other cations as well as that of anions in the RWW sample was determined by ion chromatography and inductively coupled plasma atomic emission spectroscopy (ICP-OES) as previously reported [51].

TOC values were obtained from direct injection into a VCSN TOC analyzer from Shimadzu. Assuming the following reactions for total mineralization of MeP, EtP and PrP:

$$C_8H_8O_3 + 13H_2O \rightarrow 8\ CO_2 + 34H^+ + 34\ e^- \quad (5)$$

$$C_9H_{10}O_3 + 15H_2O \rightarrow 9\ CO_2 + 40H^+ + 40\ e^- \quad (6)$$

$$C_{10}H_{12}O_3 + 17H_2O \rightarrow 10\ CO_2 + 46H^+ + 46\ e^- \quad (7)$$

and considering that equimolar mixtures were always prepared, the average number of electrons was $n = 40$, whereas the average number of C atoms was $m = 9$. Hence, the mineralization current efficiency (MCE) for each trial was estimated as follows [21]:

$$\%MCE = \frac{nFV_s\Delta(TOC)_{exp}}{4.32 \times 10^7 mIt} \times 100 \quad (8)$$

where F is the Faraday constant (96,485C mol^{-1}), V_s is the solution volume (L), $\Delta(TOC)_{exp}$ is the experimental TOC decay (mg C L^{-1}), 4.32×10^7 is a conversion factor to homogenize the units, I is the applied current (A) and t is the electrolysis time (h).

The specific energy consumption per unit TOC mass (EC_{TOC}) was estimated as follows [21]:

$$EC_{TOC}(kWh(kgTOC)^{-1}) = \frac{1000E_{cell}It}{V_s\Delta(TOC)_{exp}} \quad (9)$$

where E_{cell} is in V and the rest of parameters has been already defined. The average E_{cell} value in each system is given in Table S1 of Supplementary Material.

The concentration decay of MeP, EtP and PrP was assessed by reversed-phase HPLC on a Waters 600 LC fitted with a BDS Hypersil C18 6 μm, 250 mm × 4.6 mm, column at 35 °C and coupled to a Waters 996 PDA detector set at each maximum wavelength in the UV region. Most of the samples were conveniently diluted with acetonitrile and/or mixed with sodium thiosulfate to prevent further degradation once withdrawn upon electrolysis. A 40:60 (v/v) acetonitrile/water mixture was eluted at 1 mL min^{-1} as mobile phase, yielding perfectly symmetric peaks at 5.2, 7.1 and 10.7 min related to MeP, EtP and PrP, respectively. Linear carboxylic acids were identified by ion-exclusion HPLC using the same chromatograph fitted with a Bio-Rad Aminex HPX 87H, 300 mm x 7.8 mm, column at 35 ° C, and setting the detector at λ = 210 nm. A 4 mM H_2SO_4 solution was eluted at 0.6 mL min^{-1} as mobile phase, yielding peaks at 6.7, 9.6 and 13.9 min for oxalic, malic and formic acid, respectively.

The main primary aromatic by-products formed in the absence and presence of Cl^- were identified by treating mixtures of the three parabens (0.30 mM each) in either 5 mM Na_2SO_4 or RWW by SPEF for 10, 30, 60 and 240 min. The organic components contained in 50 mL of electrolyzed samples were concentrated using solid-phase extraction tips (Agilent Bond Elute OMIX SPE), followed by elution with 2 mL of methanol. After concentration down to 1 mL with a gentle N_2 stream, the final samples were analyzed by gas chromatography-mass spectrometry (GC–MS). An Agilent Technologies system composed of a 6890N chromatograph coupled to a 5975 XL mass spectrometer, operating in electron ionization mode at 70 eV, was employed. A non-polar Teknokroma Sapiens-X5.ms 0.25 μm, 30 m × 0.25 mm, column was used, with the following temperature ramp: 36 °C for 1 min, 5 °C min^{-1} up to 320 °C and hold time 10 min. The temperature of the inlet, source and transfer line was 250, 230 and 280 °C. A NIST05 MS library allowed the identification of the mass spectra.

3. Results and discussion

3.1. Treatment of mixtures of parabens in Na_2SO_4 using a BDD/air-diffusion cell

As a preliminary investigation, the performance of various EAOPs was assessed in a synthetic aqueous matrix containing Na_2SO_4 as single electrolyte. This kind of study has been usually made in acidic solutions with high conductivity (i.e., 0.050 M Na_2SO_4) [21,24], but in the present work the electrolyses were carried out in a 5 mM Na_2SO_4 solution at pH 3.0 aiming to mimic the low conductivity of real effluents from WWTFs (~ 3.70 mS cm^{-1} after pH adjustment). A pre-pilot plant with a BDD/air-diffusion cell was employed to treat solutions of 2.5 L at a j as low as 10 mA cm^{-2} due to the low conductivity.

The ability of the flow cell to electrogenerate H_2O_2 under different conditions is depicted in Fig. S1 of Supplementary Material. In the absence of Fe^{2+} in the dark (EO-H_2O_2 conditions), a continuous accumulation of H_2O_2 from Reaction (2) was observed, attaining 4.2 mM at 240 min. The accumulation rate diminished over time, as a result of the progressively larger destruction of H_2O_2 by oxidation at the BDD surface. Worth mentioning, the electrogeneration at such low j was more efficient than that reported elsewhere at high j; for example, 8.0 mM H_2O_2 was accumulated at 240 min in 0.050 M $HClO_4$ at 50 mA cm^{-2} [31]. This means that at low j, parasitic reactions like reduction of H_2O_2 to H_2O and H^+ to H_2 are minimized. A much lower steady H_2O_2 concentration of ~ 2.4 mM was reached from 60 min working in the presence of 0.20 mM Fe^{2+} (EF conditions), once the H_2O_2 production was perfectly counterbalanced by its destruction at the anode surface and in the bulk. In general, 0.5-1.0 mM Fe^{2+} is added to promote Fenton's Reaction (3) in systems with an air-diffusion cathode [1], but a lower catalyst concentration seems enough at low j. This is interesting aiming to further propose the treatment of RWW, where the addition of iron must be limited from an economic and environmental standpoint. Finally, an analogous electrolysis but under solar irradiation (SPEF conditions) yielded a lower accumulation of 1.4 mM H_2O_2 at 240 min. This is explained by the continuous photoreduction of Fe(III), produced via Fenton's Reaction (3), to Fe^{2+} from Reaction (4), accelerating the destruction of H_2O_2 in the bulk. As a result, the *in situ* production of ·OH in the bulk at low j was enhanced in the order EO-H_2O_2 ≪ EF ≪ SPEF.

Next, the ability of the three EAOPs to degrade equimolar mixtures of three parabens (0.30 mM each) in 5 mM Na_2SO_4 at pH 3.0 was compared. Fig. S2a, c and e of Supplementary Material shows the concentration decay of MeP, EtP and PrP with electrolysis time. In EO-H_2O_2 (Fig. S2a), about 65% of parabens removal was achieved at 360 min upon reaction with BDD(·OH) formed in the anode vicinity from Reaction (1). No substantial difference could be appreciated between the three profiles. However, the corresponding pseudo-first-order kinetic analysis of Fig. S2b highlights a slightly higher slope for PrP compared to MeP and EtP. This is more evident from the apparent rate

Table 1
Pseudo-first-order rate constant for methylparaben (k_{MeP}), ethylparaben (k_{EtP}) and propylparaben (k_{PrP}), along with the corresponding *R*-squared, obtained upon degradation of 2.5 L of equimolar mixtures (0.30 mM each) in different matrices at pH 3.0 using a pre-pilot plant containing a cell with an air-diffusion cathode under selected conditions.

Anode	Process	Medium[a]	j (mA cm^{-2})	k_{MeP} (min^{-1})	R^2	k_{EtP} (min^{-1})	R^2	k_{PrP} (min^{-1})	R^2
BDD	EO-H_2O_2	5-S	10	2.5×10^{-3}	0.997	2.6×10^{-3}	0.995	3.1×10^{-3}	0.987
	EF[b]	5-S	10	0.013	0.991	0.013	0.994	0.012	0.997
	SPEF[b]	5-S	10	0.021	0.993	0.020	0.996	0.020	0.998
	SPEF[b]	SWM	10	0.019	0.982	0.019	0.987	0.018	0.994
	SPEF[b]	RWW	10	0.026	0.980	0.025	0.980	0.025	0.985
RuO_2-based	SPEF[b]	5-S	10	0.014	0.993	0.014	0.992	0.012	0.996
	SPEF[b]	SWM	10	0.011	0.982	0.011	0.988	0.011	0.995
	SPEF[b]	RWW	5	7.2×10^{-3}	0.984	7.3×10^{-3}	0.993	7.7×10^{-3}	0.995
	SPEF[b]	RWW	10	0.018	0.983	0.017	0.987	0.018	0.992
	SPEF[b]	RWW	20	0.025	0.981	0.025	0.983	0.024	0.980
	SPEF[b]	RWW	30	0.031	0.985	0.030	0.987	0.030	0.987
	SPEF[c]	RWW	10	0.020	0.996	0.020	0.997	0.019	0.996

[a] 5-S: 5 mM Na_2SO_4; SWM: simulated water matrix; RWW: real wastewater.
[b] 0.20 mM Fe^{2+} added to the solution.
[c] 0.50 mM Fe^{2+} added to the solution.

constants summarized in Table 1, showing that $k_{PrP} = 3.1 \times 10^{-3}\,min^{-1} \gg > k_{MeP} \sim k_{EtP} \sim 2.6 \times 10^{-3}\,min^{-1}$, which suggests the occurrence of a larger adsorption of PrP on BDD. A much quicker decay, with total disappearance of all parabens at 360 min despite the low *j*, was found in EF with 0.20 mM Fe^{2+}, as can be seen in Fig. S2c. In this process, no difference could be observed between the three degradation profiles, meaning that ·OH formed in the bulk was the main oxidant. The corresponding kinetic analysis presented in Fig. S2d yielded the rate constants included in Table 1, with a mean value of 0.013 min^{-1}. A dramatic acceleration of the parabens degradation was achieved in SPEF with 0.20 mM Fe^{2+}. As shown in Fig. S2e, only 180 min were required to completely remove MeP, EtP and PrP, which is confirmed by the much greater mean rate constant of 0.020 min^{-1} (see Fig. S2f and Table 1). The outstanding contribution of continuous Fe^{2+} regeneration and additional ·OH production from photo-Fenton Reaction (4) upon sunlight irradiation is confirmed, eventually enhancing the ·OH production from Fenton's Reaction (3).

TOC abatement for the same three trials is illustrated in Fig. S3 of Supplementary Material. In EO-H_2O_2, 35% mineralization was attained after 240 min. Since a low amount of BDD(˙OH), the only oxidant in this process, was produced at 10 mA cm^{-2}, the gradual degradation of reaction by-products occurred very slowly. In fact, note that 50% of the initial parabens content was still present in solution (Fig. S2a). A very similar TOC decay was achieved in EF, ending in a close TOC value at 240 min. This means that ·OH produced from Fenton's Reaction (3) can easily oxidize the parent pollutants (Fig. S2c), but not the very refractory complexes formed between Fe(III) and organic intermediates like linear carboxylic acids. Such complexes can be typically degraded by BDD(˙OH), but its concentration was too small at low *j*, as mentioned before. A substantially larger mineralization of 51% was attained in SPEF. This may be explained by the crucial role of high power UV light from natural sunlight, which promoted: (i) the production of larger quantities of ·OH, induced by photo-Fenton Reaction (4), as mentioned above (Fig. S2e), and (ii) the more decisive photodecarboxylation of refractory Fe(III)-carboxylate complexes as follows [1]:

$$Fe(OOCR)^{2+} + h\nu \rightarrow Fe^{2+} + CO_2 + R\cdot \quad (10)$$

Therefore, sunlight irradiation ensured the progressive TOC decay despite the low input current. Fig. S4 of Supplementary Material highlights the kind of aliphatic by-products, mostly present as Fe(III) complexes [1], that were accumulated during the above SPEF degradation of the parabens mixture. Oxalic acid was accumulated at a very small concentration (≪ 5 mg L^{-1}) during the whole electrolysis, owing to the very effective photodegradation of the Fe(III)-oxalate complexes [24]. In contrast, a much larger accumulation was found for malic acid, attaining 66 mg L^{-1} as maximal at 120–150 min. Later, the concentration progressively decayed down to 46 mg L^{-1} since it was more quickly destroyed than formed, in agreement with the small amount of remaining parabens (precursors of carboxylic acids) at that time (Fig. S2e). Note that malic acid only accounted for 16 mg L^{-1} TOC at 240 min, which is only a 33% of the solution TOC (Fig. S3), suggesting that other kinds of refractory by-products were also accumulated.

3.2. SPEF treatment in real wastewater matrix using a BDD/air-diffusion cell

Once the degradation ability of the three EAOPs was corroborated at low *j* in a simple aqueous matrix, the same pre-pilot flow plant and cell were employed to degrade mixtures of the three mentioned parabens (0.30 mM each) in the presence of 0.20 mM Fe^{2+} at pH 3.0 by SPEF at 10 mA cm^{-2} in SWM or RWW. The initial TOC was 100 mg L^{-1} in SMW, whereas it was ~ 110 mg L^{-1} in RWW due to the presence of natural organic matter (NOM).

Fig. 1 informs about the time course of the concentration of H_2O_2 and active chlorine accumulated along the SPEF treatment in each medium. H_2O_2 was formed via Reaction (2) gradually increasing its content up to a steady value from 120 min. At 240 min, 1.45 and 1.85 mM was attained in SWM and RWW, respectively. On the other hand, the final active chlorine concentration arising from Cl^- oxidation at the BDD anode surface was 1.40 and 1.55 mg L^{-1} in SWM and RWW,

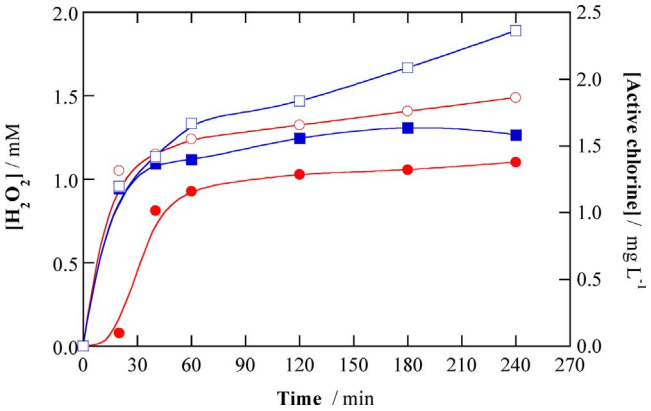

Fig. 1. Time course of the concentration of (○, □) H_2O_2 and (●, ■) active chlorine accumulated during the SPEF treatment of 2.5 L of a mixture of methylparaben, ethylparaben and propylparaben (0.30 mM each) in (○,●) simulated water matrix and (□,■) real wastewater, with 0.20 mM Fe^{2+} at pH 3.0, using a pre-pilot flow plant with a BDD/air-diffusion cell of 20 cm^2 electrode area at current density (*j*) of 10 mA cm^{-2} and 30 °C.

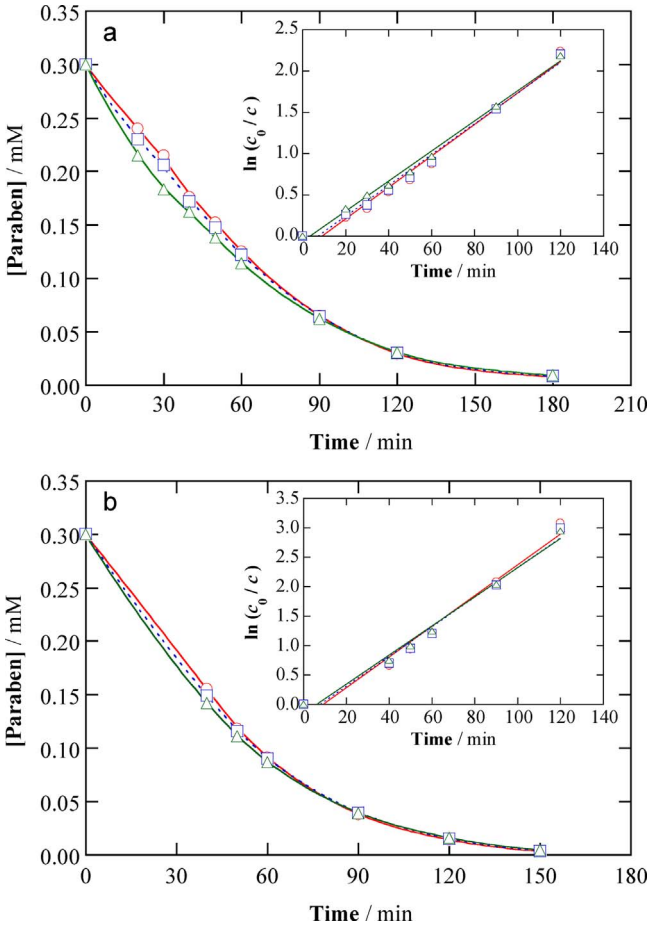

Fig. 2. Concentration decay of (◯) methylparaben, (□) ethylparaben and (△) propylparaben with electrolysis time during the degradation of 2.5 L of an equimolar mixture (0.30 mM each) in (a) simulated water matrix and (b) real wastewater, with 0.20 mM Fe^{2+} at pH 3.0, by SPEF using a pre-pilot plant with a BDD/air-diffusion cell at j = 10 mA cm^{-2} and 30 °C. The inset panels present the corresponding pseudo-first-order kinetic analysis.

respectively. A higher accumulation of both oxidants was then obtained in RWW, which can be explained by the easier reaction of active chlorine with H_2O_2 according to Reaction (11) in SWM [48], which leads to a smaller steady concentration of both species compared to RWW. In this latter matrix, the oxidation of additional NOM with ·OH and HClO interferes and makes Reaction (11) more difficult.

$$HClO + H_2O_2 \rightarrow Cl^- + O_{2(g)} + H_2O + H^+ \quad (11)$$

Fig. 2 shows the decay of MeP, EtP and PrP concentration with electrolysis time during the same trials. According to Fig. 2a, total removal of the three parabens in SWM occurred at 180 min, presenting almost identical profiles to those in 5 mM Na_2SO_4 (Fig. S2). This was corroborated from the rate constants obtained from the kinetic analysis shown in the inset, yielding an average value of 0.019 min^{-1} (Table 1) that practically coincided with that found in Na_2SO_4. Hence, it can be concluded that the presence of Cl^- was not beneficial, which is in contrast to findings reported in literature. For example, the formation of active chlorine accelerated the removal of the naproxen by Fenton-based EAOPs [31]. This apparent contradiction can be related to the really small amount of chlorine generated at low j (Fig. 1) and thus, the main reactive species to justify the degradation of parabens in SWM also corresponded to ·OH formed from Fenton's Reaction (3), greatly promoted upon sunlight irradiation. This evidence allows discarding a substantial contribution of a recently suggested Fenton-like Reaction [32,52]:

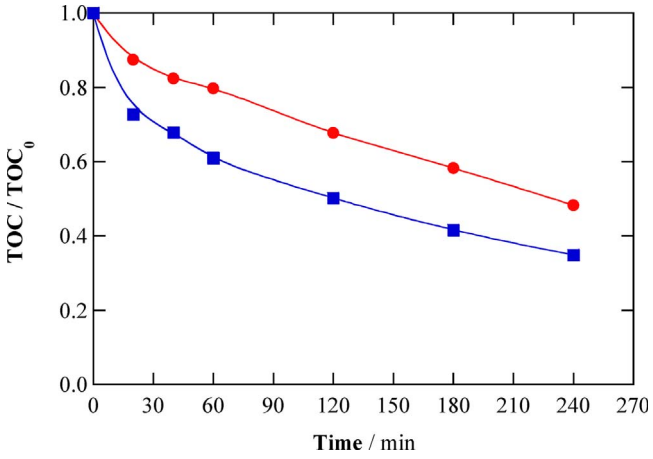

Fig. 3. Normalized TOC removal vs. electrolysis time for the SPEF treatments of Fig. 2 using (●) simulated water matrix and (■) real wastewater.

$$HClO + Fe^{2+} \rightarrow Fe^{3+} + \cdot OH + Cl^- \quad (12)$$

A faster disappearance of MeP, EtP and PrP was achieved in RWW, as can be observed in Fig. 2b, requiring 150 min for total concentration decrease. These decays were quicker than in the other two matrices, being corroborated from the linear fittings of the inset that yielded a rate constant of 0.025 min^{-1} on average (Table 1). This can be explained by: (i) the superior regeneration of Fe^{2+} from photoreduction of Fe(III) complexes formed with natural organic matter compared to that from photo-Fenton Reaction (4), and (ii) the possible formation of reactive species upon photolysis of the RWW matrix. The additional production of ·OH from Reaction (12), plausible considering the higher HClO content compared to that of SWM (Fig. 1), was probably much less relevant.

Normalized TOC abatement for these trials is depicted in Fig. 3. In SWM, 52% mineralization was reached at 240 min. This percentage as well as the trend are very similar to those obtained in 5 mM Na_2SO_4, confirming the minor role of active chlorine. This is in contrast to typical studies at high j, where the formation of free and complexed chloro-organics causes the deceleration of TOC removal due to their refractoriness to M(·OH) and ·OH [53], and can be explained by the very low content of active chlorine formed at low j. The minimization of chloroderivatives is then a very positive outcome from SPEF treatment at low input current. On the other hand, in RWW, up to 66% TOC abatement could be attained at the end of the electrolysis, which is in agreement with the aforementioned superior photoreductive and photolytic effects of sunlight in the presence of NOM. It is worth to mention that, at high j, the presence of such organic matter is rather detrimental [53], because it acts as a radical scavenger consuming M(·OH) and ·OH. As a result, it is more quickly destroyed, thus minimizing the formation of photosensitive complexes with Fe(III) that constitute a source of Fe^{2+}.

To end with the investigation using the BDD/air-diffusion cell, the current efficiency and energy consumption were calculated from Eq. (8) and (9), respectively, since these parameters may be better indicators to show the positive impact of low j in electrochemical treatments. Fig. 4 compares the trends of MCE and EC_{TOC} for the SPEF treatment of mixtures of MeP, EtP and PrP (0.30 mM each) in the three media mentioned above, at j = 10 mA cm^{-2}. The maximum efficiencies in all matrices were achieved during the early stages, as can be seen in Fig. 4a. MCE values of 380%, 450% and up to 1000% were determined in 5 mM Na_2SO_4, SWM and RWW, respectively. Such impressive MCE has never been reported so far, and can be related to: (i) a very efficient action of ·OH at low j generated from Fenton's Reaction (3) upon minimization of parasitic reactions, which was enormously empowered by photolytic Reaction (4), combined with (ii) the great photoreductive

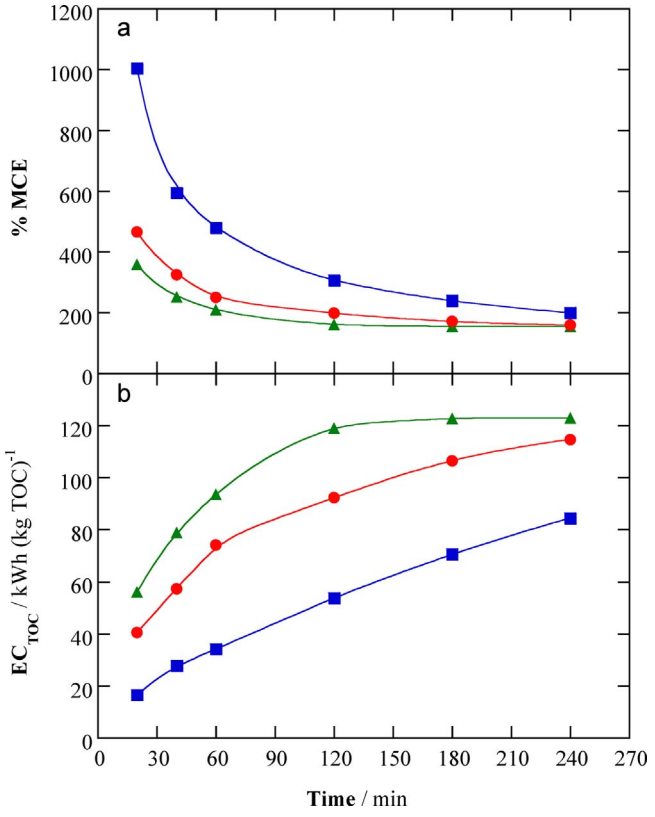

Fig. 4. Change of (a) mineralization current efficiency and (b) specific energy consumption per unit TOC mass with electrolysis time for the SPEF treatment of 2.5 L of 0.30 mM methylparaben + 0.30 mM ethylparaben + 0.30 mM propylparaben in (▲) 5 mM Na_2SO_4, (●) simulated water matrix and (■) real wastewater, all with 0.20 mM Fe^{2+} of pH 3.0, using a pre-pilot plant equipped with a BDD/air-diffusion cell at j = 10 mA cm^{-2} and 30 °C.

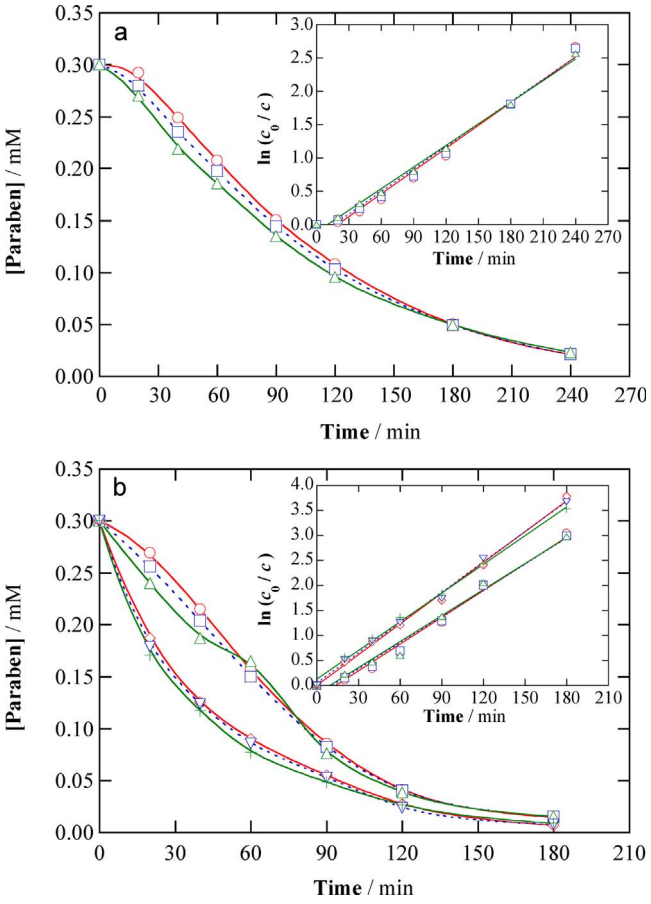

Fig. 5. Concentration abatement of (○,◇) methylparaben, (□,▽) ethylparaben and (△,+) propylparaben vs. electrolysis time for the treatment of 2.5 L of an equimolar mixture (0.30 mM each) in (a) simulated water matrix and (b) real wastewater at pH 3.0 by SPEF using a pre-pilot plant with a RuO_2-based/air-diffusion cell at j = 10 mA cm^{-2} and 30 °C. [Fe^{2+}] = (○, □,△) 0.20 mM and (◇,▽,+) 0.50 mM. The pseudo-first-order kinetic analysis is shown in the insets.

and photolytic effect of sunlight on Fe(III) complexes, mainly with those formed with final carboxylic acids that are efficiently and rapidly photodecomposed via Reaction (10). The higher efficiency in RWW and the similarity between trials in SWM and Na_2SO_4 media are in agreement with TOC decays (Fig. S3 and 3). The progressive decay of MCE over time was due to decrease of organic load upon mineralization and the larger refractoriness of by-products, although an MCE as high as 200% was still obtained at 240 min. As expected, the EC_{TOC} trends with electrolysis time presented the opposite behavior, with higher consumption in the order RWW ≪ SWM ~ Na_2SO_4. Much lower consumptions compared to previous studies, i.e., 54, 110 and 123 kWh (kg TOC)$^{-1}$, were required in the above media for 50% TOC reduction, respectively. For example, EC_{TOC} = 2400 kWh (kg TOC)$^{-1}$ resulted from SPEF treatment of pesticide tebuthiuron in 0.050 M Na_2SO_4 with 0.50 mM Fe^{2+} at pH 3.0 using a BDD/air-diffusion cell at j = 50 mA cm^{-2} [21]. SPEF with BDD anode at low j is then very effective and extraordinarily efficient, being particularly well suited for treatments in real water matrices.

3.3. SPEF treatment in real wastewater matrix using a RuO_2-based/air-diffusion cell

Once verified the very good results applying SPEF with BDD, the interest was to replace this anode by a less expensive RuO_2-based anode so as to assess if the system could maintain an acceptable performance.

First, the ability of the RuO_2-based/air-diffusion cell to electrogenerate H_2O_2 and active chlorine on site was tested during the SPEF treatment of 2.5 L of a mixture of 0.30 mM MeP + 0.30 mM EtP + 0.30 mM PrP in RWW with 0.20 mM Fe^{2+} at pH 3.0 and j = 10 mA cm^{-2}, yielding the concentrations depicted in Fig. S5 of Supplementary Material. The H_2O_2 content increased up to a steady concentration of 3.5 mM already reached at 90–120 min. Note the larger value obtained as compared to that with the BDD/air-diffusion cell (Fig. 1), which can be justified by the lower destruction of H_2O_2 at the RuO_2-based surface. On the other hand, active chlorine was accumulated up to 1.3 mg L^{-1}, a similar quantity to that observed with the other cell, which allows concluding that the role of this oxidant during the treatment of parabens with the metal oxide anode is also of minor importance under the present conditions.

Fig. 5a shows the concentration abatement of each paraben by SPEF in SWM with 0.20 mM Fe^{2+} at pH 3.0 and j = 10 mA cm^{-2}. Almost total decay (≫ > 95%) was attained after 240 min, with no substantial difference among the three profiles, which confirms the prevailing role of ·OH formed from Fenton's Reaction (3). From the good fittings considering a pseudo-first-order kinetic analysis shown in the inset, a mean k = 0.011 min^{-1} was determined (Table 1). In RWW, Fig. 5b highlights that a shorter time of 180 min was needed for attaining ≫ > 95% removal by applying SPEF with 0.20 mM Fe^{2+}. Again, a unique k ~ 0.018 min^{-1} (Table 1) was obtained for the three molecules, which were destroyed faster compared to SPEF in SWM owing to the aforementioned key influence of sunlight irradiation. It can be inferred that, in both media, SPEF with the RuO_2-based anode was slower than using BDD (Fig. 2). This allows concluding that the contribution of M(·OH) cannot be completely disregarded at low j, in contrast to previous findings in SPEF at high j where the oxidation power of SPEF was independent of the anode nature, as in the case of salicylic acid [54]. For comparison, trials in 5 mM Na_2SO_4 were also carried out (Table 1),

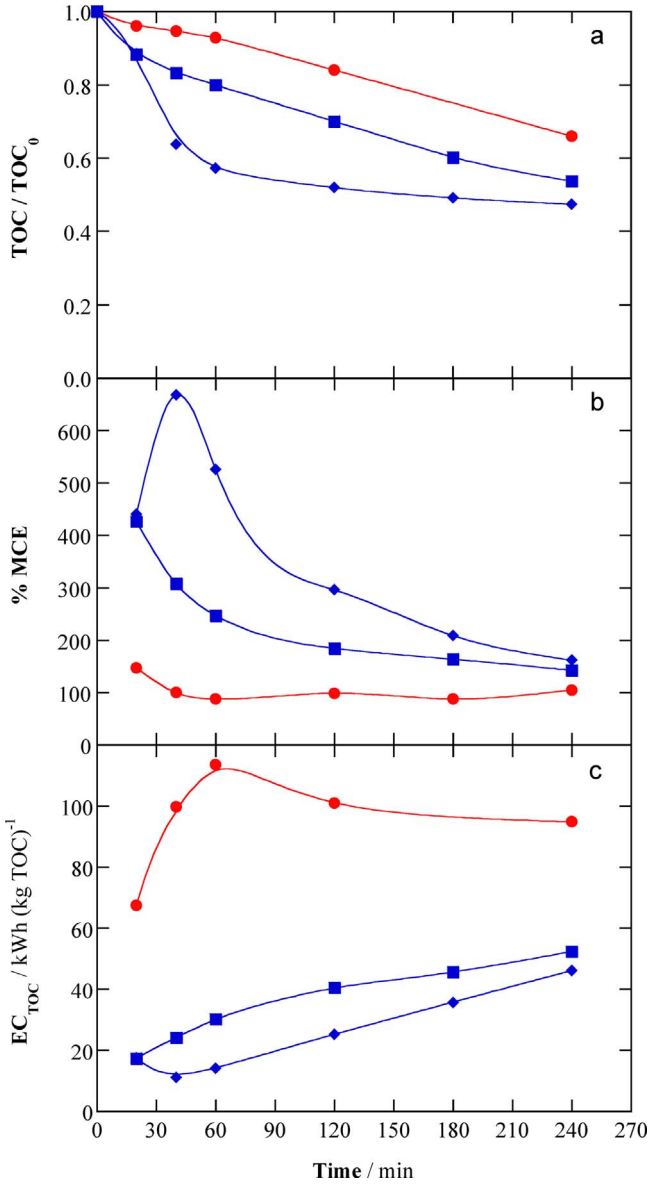

Fig. 6. Time course of (a) normalized TOC, (b) mineralization current efficiency and (c) specific energy consumption per unit TOC mass during the SPEF treatments of Fig. 5. (●) Simulated water matrix with 0.20 mM Fe^{2+}, and real wastewater with (■) 0.20 and (◆) 0.50 mM Fe^{2+}.

yielding similar results to those commented in SWM as occurred with the BDD/air-diffusion cell.

The effect of Fe^{2+} concentration is also investigated in Fig. 5b. The use of 0.50 mM Fe^{2+} led to a substantially quicker disappearance of all parabens until 90 min, which can be accounted for by the acceleration of Fenton's Reaction (3) producing larger quantities of ·OH. However, an almost analogous decay was finally attained at 180 min, thus yielding $k = 0.020\ min^{-1}$ (Table 1) that was similar to that at 0.20 mM Fe^{2+}. This was due to the complexation of iron ions, which required some time to be photoreduced to free Fe^{2+}.

Normalized TOC abatements with electrolysis time for the same trials of Fig. 5 are shown in Fig. 6a. In SWM, 35% mineralization was achieved after 240 min. A quite faster TOC decay can be observed during all the electrolysis in RWW with 0.20 mM Fe^{2+}, reaching 47%. This agrees with the superiority of SPEF in RWW commented in Fig. 5. If compared with Fig. 3, showing 52% and 66% mineralization in SWM and RWW, respectively, it is evident that the RuO_2-based/air-diffusion cell exhibited a lower oxidation power, reinforcing the idea that the oxidizing role of M(·OH) cannot be disregarded. Worth mentioning, the progressive deceleration of TOC removal along the treatment, which is partly due to formation of more recalcitrant by-products, precludes a significant accumulation of chloroderivatives, as deduced from the poor production of active chlorine (Fig. S5). Fig. 6a also shows that the addition of a higher amount of Fe^{2+} catalyst (0.50 mM) to perform SPEF in RWW clearly upgraded the treatment at the beginning, thanks to the faster production of hydroxyl radicals. However, the enhancement at 240 min (final mineralization of 52%) was so little that the 0.20 mM Fe^{2+} can be considered as optimal. The MCE and EC_{TOC} profiles from all these TOC analyses are gathered in Fig. 6b and c, respectively. A constant MCE of 100% was determined in SWM during the whole electrolysis. Much more efficient treatments were obtained in RWW, starting at about 425% and decaying down to 142% after 240 min. SPEF with 0.50 mM Fe^{2+} was slightly more efficient, attaining 675% as maximal. In correspondence with these trends, the EC_{TOC} values were greater in SWM, being near 95 kWh $(kg\ TOC)^{-1}$ versus only 11 kWh $(kg\ TOC)^{-1}$ in RWW for 35% TOC reduction. From comparison with the BDD/air-diffusion cell (Fig. 4c), it can be observed that much lower energy was consumed with the RuO_2-based anode, due to the remarkably lower E_{cell} (Table S1).

Although a relatively high concentration of parabens has been employed in all the above assays, aiming at providing an accurate assessment of the degradation ability of SPEF treatment, it is interesting to evaluate the performance of this technology to remove more realistic contents. The effect of parabens concentration is shown in Fig. 7a for the SPEF degradation of an equimolar mixture (30 μM each) in RWW with 0.20 mM Fe^{2+} at pH 3.0 and $j = 10\ mA\ cm^{-2}$. At 180 min, the removal was ≫ > 95% for MeP, 88% for EtP and 60% for PrP. The much slower abatement compared to previous trials at 0.30 mM of each paraben can be explained by the greater mass transport limitations

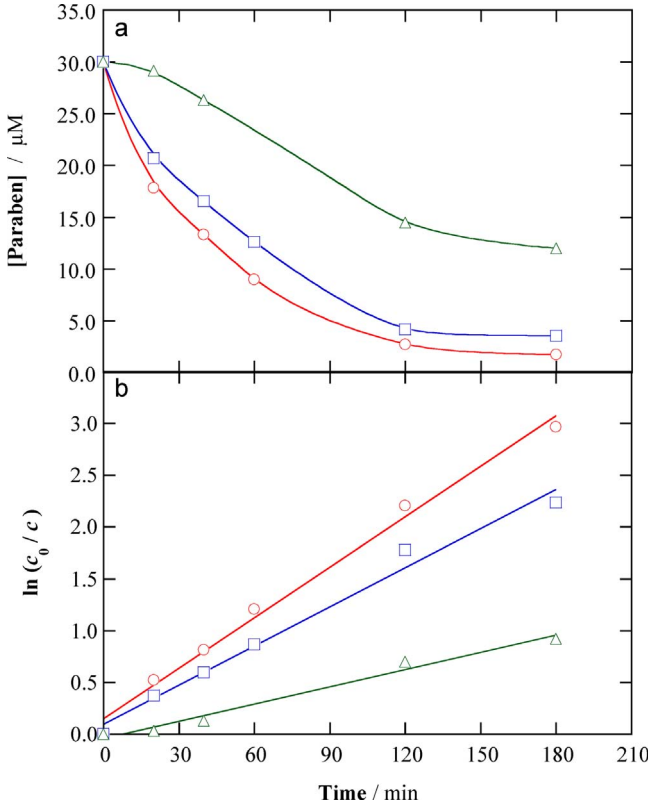

Fig. 7. (a) Variation of the concentration of (○) methylparaben, (□) ethylparaben and (△) propylparaben with electrolysis time for the SPEF degradation of an equimolar mixture (30 μM each) in real wastewater with 0.20 mM Fe^{2+} at pH 3.0 using a pre-pilot plant with a RuO_2-based/air-diffusion cell at $j = 10\ mA\ cm^{-2}$ and 30 °C. (b) Pseudo-first-order kinetic analysis of concentration decays.

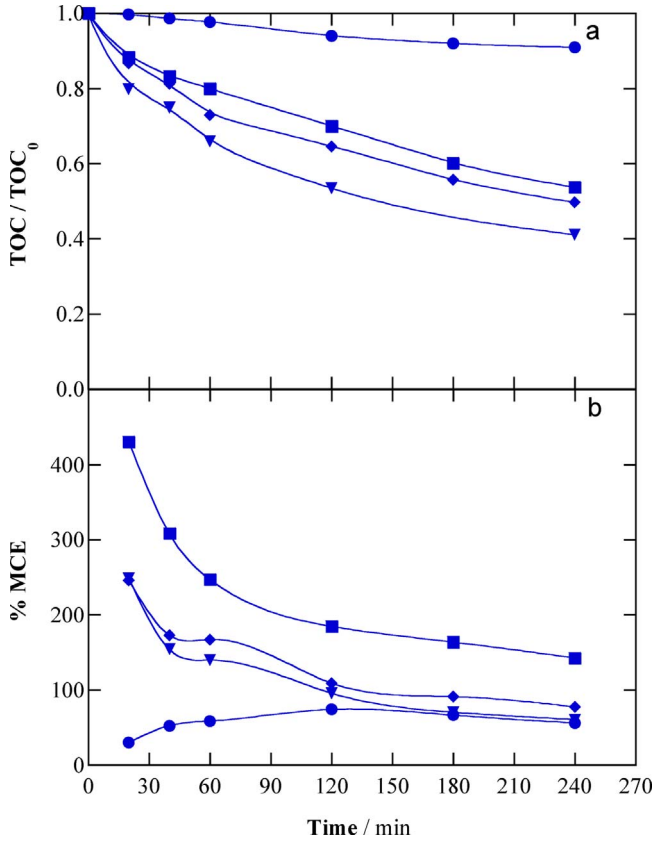

Fig. 8. (a) Normalized TOC removal and (b) mineralization current efficiency with electrolysis time during the SPEF treatment of 2.5 L of a mixture containing 0.30 mM methylparaben + 0.30 mM ethylparaben + 0.30 mM propylparaben in real wastewater with 0.20 mM Fe^{2+} at pH 3.0 and 30 °C using a pre-pilot plant with a RuO_2-based/air-diffusion cell at j = (●) 5 mA cm^{-2}, (■) 10 mA cm^{-2}, (◆) 20 mA cm^{-2} and (▼) 30 mA cm^{-2}.

inherent to low concentrations of organics, whose reactive events with oxidants become substantially limited. Under these conditions, the treatment is less efficient because M(·OH) and ·OH are largely consumed in parasitic reactions. Fig. 7b reveals that even at such low content of pollutants, the decays agreed well with a pseudo-first-order kinetics, yielding $k_{MeP} = 0.016\ min^{-1} \gg > k_{EtP} = 0.013\ min^{-1} \gg > k_{PrP} = 5.6 \times 10^{-3}\ min^{-1}$. Hence, in this case the length of the side chain of each paraben had influence on reactivity, which can be justified by the gradually lower diffusion rate to meet the M(·OH) and ·OH.

For the final optimization of the SPEF treatment of parabens mixtures in RWW with 0.20 mM Fe^{2+} at pH 3.0, the influence of applied j was studied within the range 5–30 mA cm^{-2}. From Table 1, it is evident that the pseudo-first-order rate constant for MeP, EtP and PrP gradually increased as j was raised, as expected from the faster production of H_2O_2 that ended in a greater amount of ·OH from Fenton's Reaction (3) as well as from the quicker generation of M(·OH) from Reaction (1). Thanks to the promotion of larger quantities of oxidants, an analogous upgrade with increasing j was observed for normalized TOC removal (TOC_0 = 110 mg L^{-1}) in Fig. 8a, attaining 10%, 47%, 51% and 59% mineralization at 5, 10, 20 and 30 mA cm^{-2}, respectively. In order to evaluate the convenience of using a high j, the corresponding MCE profiles were determined. As shown in Fig. 8b, the efficiency was always lower than 100% at 5 mA cm^{-2}, thus giving rise to the less powerful and less efficient SPEF treatment owing to the poor generation of M(·OH) and ·OH. A quite higher MCE was found at 10 mA cm^{-2}, as commented above. This j became optimal in terms of efficiency, since at 20 and 30 mA cm^{-2} the maximum MCE value was around 250%, further decreasing down to 100% at 240 min. In conclusion, the slightly larger percentage of mineralization at $j \gg > 10$ mA cm^{-2} did not counterbalance the much lower efficiency and hence, the higher electrical cost.

3.4. Reaction pathways upon SPEF treatment at low input current

Four main primary intermediates were detected by GC–MS during the SPEF degradation of a mixture of the three parabens in 5 mM Na_2SO_4 or RWW, always with 0.20 mM Fe^{2+} at pH 3.0, using a BDD/air-diffusion cell at constant j values. The results were verified employing a RuO_2-based/air-diffusion cell.

Depending on the sampling time, residual amounts of MeP (m/z 152), EtP (m/z 166) and PrP (m/z 180) could be found at 23.8, 24.1 and 26.2 min, respectively. In Na_2SO_4 medium, three by-products were identified: *p*-hydroxybenzoic acid (m/z 138) at 14.2 min, formed upon hydroxylation of each paraben on the carbonyl group; 3,4-dihydroxy ehtylbenzoate (m/z 182) at 30.4 min, which may appear under the attack of M(·OH) and ·OH over the aromatic ring of EtP and could be subsequently transformed into *p*-hydroxybenzoic acid; and 3,4-dihydroxybenzoic acid (m/z 154) at 32.4 min, resulting from the additional hydroxylation of the benzenic ring of *p*-hydroxybenzoic acid. In RWW, the additional formation of an organochlorinated by-product, namely 2,4,6-trichlorobenzoic acid (m/z 224) at 30.8 min, was observed. This means that, despite the minor role attributed to active chlorine during the degradation of parabens at low j, its electrogeneration (Fig. 1 and S5) was able to cause the chlorination of the benzenic ring during the attack of hydroxyl radicals. In non-chlorinated media, hydroxylation of the parent paraben on the benzenic ring was also demonstrated upon application of solar photocatalysis with TiO_2 to MeP [44] and EO with BDD to EtP [47]. In our previous study on EF and PEF treatment of MeP, the formation of *p*-hydroxybenzoic acid was shown [48]. On the other hand, different chlorinated parabens were identified in electrochemical [48] and non-electrochemical [47] treatments.

To end, the ability of SPEF with the RuO_2/air-diffusion cell at 10 mA cm^{-2} to effectively mineralize parabens and their primary by-products was assessed by means of prolonged electrolyses. Fig. S6a of Supplementary Material depicts the TOC decay with electrolysis time for a SPEF trial made in two consecutive days, so as to reach 480 min under a constant natural UV irradiation from sunlight. As much as 70% TOC removal was achieved, a much greater value than 47% attained at 240 min (Fig. 6a). This means that overall mineralization would be feasible at long time using the RuO_2-based anode. The evolution of major linear-chain carboxylic acids formed during this trial can be seen in Fig. S6b of Supplementary Material. Up to 60 and 38 mg L^{-1} of malic and formic acid were accumulated, respectively, at 180–240 min, whereupon a gradual decay to very low values occurred in accordance with TOC abatement promoted by photodecarboxylation via Reaction (10). At 480 min, the residual TOC was probably due to other unidentified aliphatic by-products.

4. Conclusions

This work demonstrates that it is possible to completely decontaminate real wastewater from urban WWTFs containing mixtures of parabens by means of SPEF process with a cheap metal oxide anode. Even more relevant, this has been achieved at low j = 10 mA cm^{-2} upon addition of a small amount of Fe^{2+} as catalyst, thus resulting in extraordinarily high efficiencies up to 425% and low energy consumptions. SPEF with BDD anode performed even better, reaching 1000% of MCE but consuming much more energy owing to the higher cell voltage. As a very positive feature, the degradation was always faster in the order Na_2SO_4 ~ SWM ≪ RWW, thanks to the high UV power from natural sunlight that regenerates Fe^{2+} via efficient photoreduction of Fe(III) complexes formed with natural organic load. A j = 10 mA cm^{-2} was optimum since a lower or higher current density enhanced the parasitic reactions that wasted the M(·OH) and ·OH.

Very low concentrations of parabens could also be degraded, although the treatment was decelerated owing to the mass transport limitations. The rate constant decreased in the order $k_{MeP} \gg > k_{EtP} \gg > k_{PrP}$ because the longer side chain gradually caused a slower diffusion. The main reaction pathways involved the hydroxylation on the carbonyl group or the aromatic ring, although one chloroderivative was also identified despite the minor role of electrogenerated active chlorine.

Acknowledgments

Financial support from project CTQ2016-78616-R (AEI/FEDER, EU) is acknowledged. J. R. Steter thanks funding from process number 234142/2014-6 (CNPq, Brazil).

Appendix A. Supplementary data

Supplementary data associated with this article can be found, in the online version, at http://dx.doi.org/10.1016/j.apcatb.2017.10.060.

References

[1] I. Sirés, E. Brillas, M.A. Oturan, M.A. Rodrigo, M. Panizza, Environ. Sci. Pollut. Res. 21 (2014) 8336–8367.
[2] M.A. Oturan, J.-J. Aaron, Crit. Rev. Environ. Sci. Technol. 44 (2014) 2577–2641.
[3] X. Yu, M. Zhou, Y. Hu, K. Groenen Serrano, F. Yu, Environ. Sci. Pollut. Res. 21 (2014) 8417–8431.
[4] W. Wu, Z.-H. Huang, T.-T. Lim, Appl. Catal. A: Gen. 480 (2014) 58–78.
[5] C.A. Martínez-Huitle, M.A. Rodrigo, I. Sirés, O. Scialdone, Chem. Rev. 115 (2015) 13362–13407.
[6] A. Dirany, I. Sirés, N. Oturan, A. Özcan, M.A. Oturan, Environ. Sci. Technol. 46 (2012) 4074–4082.
[7] S. Cotillas, J. Llanos, M.A. Rodrigo, P. Cañizares, Appl. Catal. B: Environ. 162 (2015) 252–259.
[8] J. Paramo-Vargas, A. Mounserrath Estrada Camargo, S. Gutierrez-Granados, L.A. Godinez, J.M. Peralta-Hernandez, J. Electroanal. Chem. 754 (2015) 80–86.
[9] K.V. Plakas, S.D. Sklari, D.A. Yiankakis, G.Th. Sideropoulos, V.T. Zaspalis, A.J. Karabelas, Water Res. 91 (2016) 183–194.
[10] L. Liang, F. Yu, Y. An, M. Liu, M. Zhou, Environ. Sci. Pollut. Res. 24 (2017) 1122–1132.
[11] S. Randazzo, O. Scialdone, E. Brillas, I. Sirés, J. Hazard. Mater. 192 (2011) 1555–1564.
[12] A. Da Pozzo, E. Petrucci, Desalin. Water Treat. 53 (2015) 1352–1360.
[13] T. Liu, K. Wang, S. Song, A. Brouzgou, P. Tsiakaras, Y. Wang, Electrochim. Acta 194 (2016) 228–238.
[14] H. Roth, Y. Gendel, P. Buzatu, O. David, M. Wessling, J. Hazard. Mater. 307 (2016) 1–6.
[15] S. Lanzalaco, I. Sirés, M.A. Sabatino, C. Dispenza, O. Scialdone, A. Galia, Electrochim. Acta 246 (2017) 812–822.
[16] C. Salazar, C. Ridruejo, E. Brillas, J. Yáñez, H.D. Mansilla, I. Sirés, Appl. Catal. B: Environ. 203 (2017) 189–198.
[17] W. Wei, Y. Lu, H. Luo, G. Liu, R. Zhang, RSC Adv. 7 (2017) 25627–25633.
[18] C. Lizama-Bahena, A. Álvarez-Gallegos, J.A. Hernandez, S. Silva-Martinez, Desalin. Water Treat. 55 (2015) 3683–3693.
[19] S. Ellouze, S. Kessemtini, D. Clematis, G. Cerisola, M. Panizza, S. Chaâbane Elaoud, J. Electroanal. Chem. 799 (2017) 34–39.
[20] A. Cruz-Rizo, S. Gutiérrez-Granados, R. Salazar, J.M. Peralta-Hernández, Sep. Purif. Technol. 172 (2017) 296–302.
[21] F. Gozzi, I. Sirés, A. Thiam, S.C. de Oliveira, A. Machulek Jr., E. Brillas, Chem. Eng. J. 310 (2017) 503–513.
[22] R. Salazar, E. Brillas, I. Sirés, Appl. Catal. B: Environ. 115–116 (2012) 107–116.
[23] A. Thiam, I. Sirés, E. Brillas, Water Res. 81 (2015) 178–187.
[24] A. Thiam, I. Sirés, F. Centellas, P.L. Cabot, E. Brillas, Chemosphere 136 (2015) 1–8.
[25] C. Espinoza, J. Romero, L. Villegas, L. Cornejo-Ponce, R. Salazar, J. Hazard. Mater. 319 (2016) 24–33.
[26] H. Olvera-Vargas, N. Oturan, M.A. Oturan, E. Brillas, Sep. Purif. Technol. 146 (2015) 127–135.
[27] T. Pérez, I. Sirés, E. Brillas, J.L. Nava, Electrochim. Acta 228 (2017) 45–56.
[28] N. Flores, I. Sirés, J.A. Garrido, F. Centellas, R.M. Rodríguez, P.L. Cabot, E. Brillas, J. Hazard. Mater. 319 (2016) 3–12.
[29] F.C. Moreira, J. Soler, A. Fonseca, I. Saraiva, R.A.R. Boaventura, E. Brillas, V.J.P. Vilar, Appl. Catal. B: Environ. 182 (2016) 161–171.
[30] A. Thiam, E. Brillas, F. Centellas, P.L. Cabot, I. Sirés, Electrochim. Acta 173 (2015) 523–533.
[31] G. Coria, I. Sirés, E. Brillas, J.L. Nava, Chem. Eng. J. 304 (2016) 817–825.
[32] Z.G. Aguilar, E. Brillas, M. Salazar, J.L. Nava, I. Sirés, Appl. Catal. B: Environ. 206 (2017) 44–52.
[33] J. Boberg, C. Taxvig, S. Christiansen, U. Hauss, Reprod. Toxicol. 30 (2010) 301–312.
[34] P.W. Harvey, D.J. Everett, J. Appl. Toxicol. 24 (2004) 1–4.
[35] B.A.F. Hafeez, M.D.H. Maibach, Skin Ther. Lett. 18 (2013) 5–6.
[36] F.A. Andersen, Int. J. Toxicol. 27 (2008) 1–82.
[37] Y. Guo, K. Kannan, Environ. Sci. Technol. 47 (2013) 14442–14449.
[38] C. Haman, X. Dauchy, C. Rosin, J.-F. Munoz, Water Res. 68 (2015) 1–11.
[39] W. Li, Y. Shi, L. Gao, J. Liu, Y. Cai, J. Hazard. Mater. 300 (2015) 29–38.
[40] E.M. Cuerda-Correa, J.R. Domínguez, M.J. Muñoz-Peña, T. González, Ind. Eng. Chem. Res. 55 (2016) 5161–5172.
[41] R.C. Martins, M. Gmurek, A.F. Rossi, V. Corceiro, R. Costa, M.E. Quinta-Ferreira, S. Ledakowicz, R.M. Quinta-Ferreira, Water Sci. Technol. 74 (2016) 1867–1875.
[42] H. Zúñiga-Benítez, C. Aristizábal-Ciro, G.A. Peñuela, J. Taiwan Inst. Chem. Technol. 59 (2016) 380–388.
[43] H. Fang, Y. Gao, G. Li, J. An, P.-K. Wong, H. Fu, S. Yao, X. Nie, T. An, Environ. Sci. Technol. 47 (2013) 2704–2712.
[44] T. Velegraki, E. Hapeshi, D. Fatta-Kassinos, I. Poulios, Appl. Catal. B: Environ. 178 (2015) 2–11.
[45] J.R. Steter, D. Dionisio, M.R.V. Lanza, A.J. Motheo, J. Appl. Electrochem. 44 (2014) 1317–1325.
[46] J.R. Steter, R.S. Rocha, D. Dionisio, M.R.V. Lanza, A.J. Motheo, Electrochim. Acta 117 (2014) 127–133.
[47] Z. Frontistis, M. Antonopoulou, M. Yazirdagi, Z. Kilinic, I. Konstantinou, A. Katsaounis, D. Mantzavinos, J. Environ. Manage. 195 (2017) 148–156.
[48] J.R. Steter, E. Brillas, I. Sirés, Electrochim. Acta 222 (2016) 1464–1474.
[49] F.J. Welcher, 6th edition, Standard Methods of Chemical Analysis vol.2, R.E. Krieger Publishing Co. Huntington, New York, 1975 (part B).
[50] APWA, AWWA, WEF, Standard Methods for the Examination of Water and Wastewater, 21st Ed., American Public Health Association, Washington D.C, 2005 Method number 4500-Cl Chlorine (residual)–G. DPD Colorimetric Method pp. 4–67 to 4–68.
[51] A. Thiam, I. Sirés, J.A. Garrido, R.M. Rodríguez, E. Brillas, Sep. Purif. Technol. 140 (2015) 43–52.
[52] N. Kishimoto, Y. Nakamura, M. Kato, H. Otsu, Chem. Eng. J. 260 (2015) 590–595.
[53] C. Ridruejo, C. Salazar, P.L. Cabot, F. Centellas, E. Brillas, I. Sirés, Chem. Eng. J. 326 (2017) 811–819.
[54] E. Guinea, C. Arias, P.L. Cabot, J.A. Garrido, R.M. Rodríguez, F. Centellas, E. Brillas, Water Res. 42 (2008) 499–511.